Research Square

Preprints are preliminary reports that have not undergone peer review.
They should not be considered conclusive, used to inform clinical practice,
or referenced by the media as validated information.

Computed Tomography-Based Age and Sex Estimation Through Hyoid Bone Anthropometry and Radiodensity Analysis

Duran Güralp

guralp22@gmail.com

Health Sciences University Gulhane Training and Research Hospital

Hüseyin BALANDIZ

Health Sciences University Gulhane Training and Research Hospital

Uğur BOZLAR

Health Sciences University Gulhane Training and Research Hospital

Sait ÖZSOY

Health Sciences University Gulhane Training and Research Hospital

Burak KAYA

Health Sciences University Gulhane Training and Research Hospital

Research Article

Keywords: Hyoid bone, Age estimation, Sex determination, Radiodensity, Fusion

Posted Date: August 25th, 2026

DOI: https://doi.org/10.21203/rs.3.rs-10228904/v1

License: This work is licensed under a Creative Commons Attribution 4.0 International License. Read Full License

Additional Declarations: No competing interests reported.

Version of Record: A version of this preprint was published at International Journal of Legal Medicine on October 24th, 2026. See the published version at https://doi.org/10.1007/s00414-026-04054-y.

Abstract

In forensic investigations; examining skeletal remains for identification, age and sex estimation is crucial. Especially for advanced age groups where standardized methods are lacking. This study evaluates the anthropometric measurements, fusion degrees, and radiodensity of the hyoid bone across a large sample size. This retrospective study analyzed cervical vertebra CT scans of 660 randomly selected cases aged 15–80 years (2021–2024) based on specific exclusion criteria. The data were reconstructed into 3D models using 3D Slicer™ software to perform osteometric measurements, fusion staging, volume and radiodensity analyses. Morphometric and volume measurements were significantly higher in males. Radiodensity values were lower in females across all ages and particularly in older groups. The combined discriminant function analysis model correctly classified sex with 93.8% accuracy. In age estimation multivariate stepwise linear regression models explained 47.7% of the variance in females and 36% in males. This multiparametric CT-based study demonstrates that the hyoid bone exhibits pronounced sexual dimorphism in a Turkish population. Due to the limited explanatory power of age estimation models, providing an estimated age range is more reliable than an exact age. CT-based multidimensional analysis of the hyoid bone is a robust method for sex determination and a supportive tool for age estimation.

Introduction

Identification of deceased individuals is a central objective of forensic medical investigations. In highly decomposed bodies or skeletal remains, age and sex estimation can be performed by evaluating developmental and morphological changes in bones [1]. In addition, courts frequently request age estimation in both criminal and civil proceedings to determine an individual's chronological age.

In living individuals and anthropological studies, various skeletal landmarks are used for age estimation. From birth to young adulthood, skeletal ossification centers provide useful indicators. In older individuals, after skeletal growth has largely ceased, age estimation may rely on parameters such as costal cartilage calcification, cranial suture fusion, and age-related degenerative changes in joints and commonly examined bone surfaces [1].

Because no standardized formula has yet been established for age estimation in advanced age groups, research in this field remains ongoing. The hyoid bone is among the skeletal structures investigated for this purpose. Anatomically, it is a U-shaped bone located in the anterior neck at the level of the fourth cervical vertebra and plays important roles in mastication, swallowing, and respiration. Unlike most bones, it does not articulate directly with any other bone and consists of a body (corpus), two greater cornua, and two lesser cornua [2].

Previous studies have shown that anthropometric measurements of the hyoid bone provide significant information for sex determination [3]. In one study evaluating both metric measurements and fusion between the hyoid body and greater cornua, unilateral fusion was observed in females before the age of 50, whereas bilateral complete fusion was reported in all cases after 50 years of age; bone size also differed significantly between sexes [4]. Another computed tomography-based study assessing hyoid fusion and bone density found significant sex-related differences in bone density, with the most pronounced differences observed in older age groups [5]. The present study aims to evaluate the applicability of age- and sex-related changes in the hyoid bone for forensic age and sex estimation in the Turkish population using anthropometric measurements and radiodensity analysis in a large sample.

Materials and Methods

This retrospective study included 660 cases selected from 11,832 cervical vertebra CT scans acquired at Health Sciences University Gulhane Training and Research Hospital between 01.01.2021 and 31.12.2024. For each age from 15 to 80 years, 10 cases were randomly selected, consisting of five females and five males.

CT images were obtained using Canon Aquilion One (Canon Medical Systems, Otawara, Japan), Hitachi Scenaria View (Hitachi Ltd., Tokyo, Japan), and Philips Ingenuity (Philips Medical Systems, Cleveland, OH, USA) scanners. All scans were performed in helical mode with a tube voltage of 120 kV and a reference tube current of 275 mAs.

Images were excluded if slice thickness exceeded 0.625 mm, diagnostic quality was insufficient, cervical instrumentation such as rods or screws caused beam-hardening artifacts, extensive dental fillings impaired measurement quality, or fractures, structural abnormalities, or congenital anomalies were present in the cervical region. The cases were classified into seven age groups: 15–18, 19–30, 31–40, 41–50, 51–60, 61–70, and 71–80 years.

All CT-based measurements and analyses were performed using 3D Slicer™ software (version 5.10; Brigham and Women's Hospital, Boston, MA, USA). Ten osteometric parameters were assessed on the hyoid bone: corpus length (CL), corpus height (CH), proximal width (PW) and distal width (DW) of the greater cornua, greater cornu length (CML), anteroposterior length (HL), and maximum lateral width (HW). Fusion between the hyoid body and the greater cornua was staged according to the classification proposed by Fisher et al. [5] (Fig. 1). Eight measurements (CL, CH, PW, DW, and CML) were obtained from axial bone-window images and multiplanar reformatted images (Fig. 2). For three-dimensional segmentation, the Segment Editor module was used, and bone tissue was segmented with the Threshold tool using lower and upper limits of 130 HU and 3500 HU, respectively. A three-dimensional head and neck skeletal model was generated, and the hyoid bone was isolated using the scissors tool (Fig. 3). After segmentation, HL, HW, radiodensity, and volume measurements were obtained (Fig. 4). Mean HU, maximum HU, and volume values were calculated from the selected hyoid bone segment using the Segment Statistics module.

To assess intra- and inter-observer reliability, all parameters were remeasured by the same observer two weeks after the initial assessment and independently evaluated by another research assistant from the same clinic.

Statistical Analysis

Statistical analyses were performed using IBM SPSS Statistics for Windows, version 20.0 (SPSS Inc., Chicago, IL, USA). Continuous variables were presented as mean, standard deviation, and median (minimum–maximum), whereas categorical variables were summarized as percentages. The Kolmogorov–Smirnov test was used to assess normality. One-way analysis of variance (ANOVA) was used to compare parameters across age groups, and the Tukey test was applied for post hoc comparisons. Sex-based comparisons were performed using the independent samples t-test, and analysis of covariance (ANCOVA) was used to control for the effect of age. Nominal variables were compared using the Chi-square test. Associations between continuous variables were evaluated with Pearson's correlation coefficient. Age estimation was first assessed using univariate linear regression, followed by stepwise multivariate linear regression to generate sex-specific regression equations. Sex estimation was evaluated using discriminant function analysis, and both univariate and stepwise multivariate discriminant function equations were developed. Intra- and inter-observer agreement for measurements was assessed using the intraclass correlation coefficient (ICC). Statistical significance was set at $p < 0.05$.

Results

Measurement reliability was assessed using the Intraclass Correlation Coefficient (ICC), while intra- and inter-observer agreement for fusion staging was evaluated with the Kappa coefficient. Both analyses demonstrated high agreement for intra- and inter-observer assessments ($p < 0.001$).

The study included 660 patients aged 15–80 years, with an equal sex distribution of 330 females (50%) and 330 males (50%).

Right- and left-sided measurements of the greater cornua were compared to assess side-related differences. Statistically significant differences were identified for PW, DW, and CML parameters, as shown in Table 1.

Table 1
Side comparisons in hyoid bone greater cornu measurements

	Left	**Right**		
	Mean ± SD **Median (min-max)**	**Mean ± SD** **Median (min-max)**	**Test statistics**	
PW (mm)	5.39 ± 0.82 5.30 (3.66–8.64)	5.46 ± 0.82 5.35 (3.24–8.33)	t=-2.556	**0.011[d]**
DW (mm)	4.57 ± 0.76 4.55 (2.70–7.48)	4.51 ± 0.73 4.43 (2.53–7.92)	t = 2.110	**0.035[d]**
CML (mm)	30.15 ± 3.51 29.89 (6.91–40.93)	30.54 ± 3.45 30.38 (19.70-40.96)	t=-4.625	**< 0.001[d]**
d: Paired samples t-test				

Sex-based comparisons showed that all anthropometric measurements, except for the DW parameters, were significantly lower in females than in males ($p < 0.001$). This difference remained significant after controlling for age using covariance analysis (Table 2).

Table 2
Differences between sexes in measurements

	Female (n = 330)	Male (n = 330)		
	Mean ± SD **Median (min-max)**	**Mean ± SD** **Median (min-max)**	**t test**	**Covariance** **p**
CL (mm)	22.04 ± 2.10 21.97 (14.96–32.82)	26.35 ± 2.36 26.09 (19.95–35.45)	< 0.001 [b]	**< 0.001**[f]
CH (mm)	9.04 ± 1.44 8.95 (5.03–14.11)	11.07 ± 1.55 10.94 (5.25–16.65)	< 0.001 [b]	**< 0.001**[f]
Right PW (mm)	5.08 ± 0.68 5.01 (3.77–7.56)	5.71 ± 0.83 5.68 (3.66–8.64)	< 0.001 [b]	**< 0.001** [f]
Right PW (mm)	5.11 ± 0.65 5.06 (3.24–7.34)	5.82 ± 0.83 5.78 (3.41–8.33)	< 0.001 [b]	**< 0.001** [f]
Left DW (mm)	4.49 ± 0.71 4.48 (3.03–7.44)	4.64 ± 0.80 4.60 (2.70–7.48)	0.014 [b]	0.013 [f]
Right DW (mm)	4.43 ± 0.65 4.34 (2.53–6.39)	4.59 ± 0.79 4.49 (2.87–7.92)	0.004 [b]	**0.004** [f]
Left CML (mm)	28.07 ± 2.60 28.31 (19.17–38.35)	32.04 ± 3.29 31.93 (6.91–40.93)	< 0.001 [b]	**< 0.001** [f]
Right CML (mm)	28.67 ± 2.63 28.63 (19.70-36.22)	32.40 ± 3.16 32.34 (25.40-40.96)	< 0.001 [b]	**< 0.001** [f]
HL (mm)	34.61 ± 2.71 34.55 (25.25–42.48)	39.82 ± 3.13 39.90 (33.02–48.43)	< 0.001 [b]	**< 0.001** [f]
HW (mm)	41.90 ± 4.09 41.71 (31.98–54.97)	46.77 ± 5.19 46.34 (33.93–64.81)	< 0.001 [b]	**< 0.001**[f]
HU max	1226.98 ± 238.55 1238 (445–2080)	1308.83 ± 192.32 1317 (134–1788)	< 0.001 [b]	**< 0.001** [f]
Volume (mm^3)	1710.16 ± 273.13 1681 (1003–2765)	2614.03 ± 454.19 2580 (1540–3996)	< 0.001 [b]	**< 0.001** [f]
HU Mean	337.60 ± 64.32 338 (143–531)	370.63 ± 59.37 367 (237–590)	< 0.001 [b]	**< 0.001** [f]

b: Independent Samples t test

f: Covariance Analysis

Univariate discriminant function analysis for sex estimation showed that the best-performing individual parameters were volume (87.6%), CL (85.5%), HL (80.2%), and CH (76.4%) (Table 3).

Table 3
Results of univariate discriminant function analysis

Parameter	Wilk's Lambda (p)	Function Coefficient	Classification (Female)	Classification (Male)	Accuracy Rate
CL	**< 0.001**	0.447	4.398	5.256	85.50%
(Constant)	-	-10.808	-49.174	-69.954	
CH	**< 0.001**	0.667	4.019	4.923	76.40%
(Constant)	-	-6.707	-18.868	-27.955	
Left PW	**< 0.001**	1.309	8.714	9.793	67.60%
(Constant)	-	-7.067	-22.836	-28.659	
Right PW	**< 0.001**	1.336	9.128	10.388	69.50%
(Constant)	-	-7.305	-24.042	-30.932	
Left DW	0.014	1.319	7.829	8.081	53.80%
(Constant)	-	-6.03	-18.3	-19.454	
Right DW	0.004	1.371	8.325	8.632	53.30%
(Constant)	-	-6.185	-19.135	-20.519	
Left CML	**< 0.001**	0.337	3.208	3.635	76.10%
(Constant)	-	-10.158	-46.046	-58.921	
Right CML	**< 0.001**	0.343	3.38	3.82	75.20%
(Constant)	-	-10.486	-49.157	-62.6	
HL	**< 0.001**	0.341	4.018	4.623	80.20%
(Constant)	-	-12.68	-70.224	-92.732	
HW	**< 0.001**	-9.484	1.917	2.14	69.50%
(Constant)	-	0.214	-40.863	-50.742	
HU max	**< 0.001**	-5.852	0.026	0.028	57.00%
(Constant)	-	0.005	-16.727	-18.937	
Volume	**< 0.001**	0.003	0.012	0.019	87.60%
(Constant)	-	-5.769	-11.105	-25.02	
HU Mean	**< 0.001**	0.016	0.088	0.097	59.50%
(Constant)	-	-5.721	-15.567	-18.619	

In the multivariate stepwise discriminant function analysis, Box's M test for equality of covariance matrices was statistically significant (Box's M = 258.814; $p < 0.001$), indicating that the assumption of equal covariance matrices was

not satisfied. However, because the sex groups were balanced and the sample size was large relative to the number of variables, the discriminant analysis was considered sufficiently robust to this violation.

Potential multicollinearity among the variables was examined during stepwise discriminant analysis. Because each variable retained in the stepwise model must add a significant discriminant contribution beyond previously entered variables, tolerance values were monitored throughout the analysis. All tolerance values remained above 0.30 and did not fall below critical thresholds, indicating no substantial multicollinearity among the included variables and supporting the statistical reliability of the final discriminant function. The final model included 10 variables, with a canonical eigenvalue of 2.368 and a canonical correlation coefficient of 0.839. The Wilks' Lambda value was 0.297, and the function was statistically significant (χ^2=791.771; df = 10; $p < 0.001$). Cross-validation correctly classified 91.8% of male cases and 95.8% of female cases. The derived equation is presented below:

D = -13,270 + (0,156 × CL) + (0,145 × CH) – (0,176 × left DW) – (0,159 × right DW) – (0,063 × right CML) + (0,157 × HL) + (0,059 × HW) – (0,345 × fusion stage) + (0,001 × volume) + (0,002 × HU mean) D > 0 = male, D < 0 = female

Age-group comparisons were performed to evaluate whether the measurements differed significantly across age categories. Fusion stage distribution showed that stage-3 fusion was present in one case in the 15–18 age group, whereas stage 0 was the most frequent stage in this group, observed in 22 cases (55%). Fusion stage increased with advancing age, and stage 3 became the most common pattern after the age of 60 (Table 4).

Table 4
Comparison of fusion stages according to age groups

Age Groups	Stage 0	Stage 1	Stage 2	Stage 3	
	n (%)	n (%)	n (%)	n (%)	
15–18	22 (55)	17 (42.5)	-	1 (2,5)	**< 0.001** [c]
19–30	1 (0.8)	90 (75)	16 (13.3)	13 (10.9)	
31–40	-	52 (52)	30 (30)	18 (18)	
41–50	-	36 (36)	30 (30)	34 (34)	
51–60	-	21 (21)	45 (45)	34 (34)	
61–70	-	12 (12)	46 (46)	42 (42)	
71–80	-	12 (12)	41 (41)	47 (47)	
c: Chi-Square Test/Fisher's Exact test					

Age-group comparisons of anthropometric measurements showed that values in the 15–18 age group were generally lower than those in the older groups ($p < 0.001$). Mean radiodensity values decreased significantly in older age groups, particularly after the age of 60 ($p < 0.001$). No statistically significant differences were observed among age groups for volume, HW, or CH ($p > 0.5$). The detailed results are presented in Table 5.

Table 5
Comparison of measurement values among age groups

Parameter	Statistic	15–18	19–30	31–40	41–50	51–60	61–70	71–80	p
CL	Mean ± SD	21.27 ± 2.46	23.41 ± 2.77	24.06 ± 2.75	24.45 ± 2.78	25.01 ± 3.38	25.01 ± 3.38	24.76 ± 3.27	**p < 0.001**
CH	Mean ± SD	9.40 ± 1.43	10.10 ± 1.66	9.86 ± 1.94	10.07 ± 1.82	10.10 ± 1.93	10.06 ± 1.86	10.39 ± 1.74	p = 0.124
Left PW	Mean ± SD	5.13 ± 0.67	5.15 ± 0.76	5.39 ± 0.84	5.51 ± 0.80	5.32 ± 0.77	5.53 ± 0.87	5.60 ± 0.87	**p < 0.001**
Right PW	Mean ± SD	5.11 ± 0.59	5.24 ± 0.82	5.40 ± 0.79	5.55 ± 0.76	5.51 ± 0.79	5.57 ± 0.89	5,70 ± 0.85	**p < 0.001**
Left DW	Mean ± SD	4.22 ± 0.70	4.37 ± 0.68	4.53 ± 0.84	4.74 ± 0.78	4.53 ± 0.75	4.70 ± 0.72	4.69 ± 0.71	**p < 0.001**
Right DW	Mean ± SD	4.19 ± 0.62	4.34 ± 0.63	4.46 ± 0.78	4.61 ± 0.70	4.47 ± 0.74	4.65 ± 0.80	4.68 ± 0.69	**p < 0.001**
Left CML	Mean ± SD	27.60 ± 2.43	29.76 ± 3.24	30.08 ± 3.73	29.84 ± 4.00	30.43 ± 3.62	31.02 ± 3.02	30.86 ± 3.29	**p < 0.001**
Right CML	Mean ± SD	27.82 ± 2.18	29.92 ± 3.50	30.41 ± 3.53	30.63 ± 3.32	30.91 ± 3.68	31.51 ± 3.15	31.06 ± 3.31	**p < 0.001**
HL	Mean ± SD	35.15 ± 3.20	37.03 ± 3.92	36.73 ± 3.96	37.36 ± 4.09	37.74 ± 4.15	38.04 ± 3.56	37.22 ± 3.80	**p < 0.001**
HW	Mean ± SD	43.91 ± 3.67	44.61 ± 5.18	45.23 ± 6.43	44.11 ± 4.58	43.99 ± 5.20	43.82 ± 5.31	44.39 ± 5.28	p = 0.534
HU max	Mean ± SD	1254.65 ± 140.35	1307.93 ± 242.78	1318.52 ± 174.58	1277.79 ± 194.59	1258.64 ± 189.03	1250.83 ± 257.61	1181.04 ± 251.19	**p < 0.001**
Volume	Mean ± SD	1768.95 ± 358.57	2049.84 ± 511.93	2121.53 ± 535.69	2228.93 ± 578.50	2254.94 ± 610.21	2255.37 ± 620.23	2241.67 ± 665.54	p = 0.534
HU mean	Mean ± SD	373.08 ± 44.18	375.08 ± 64.68	371.66 ± 48.33	360.04 ± 56.01	354.98 ± 60.46	337.44 ± 72.02	313.72 ± 64.91	**p < 0.001**

Linear regression analyses were conducted separately for females and males to estimate age from each parameter, and the results are summarized in Table 6. In females, mean HU explained the greatest proportion of age variation ($F = 94.426$; $p < 0.001$), accounting for 22.4% of the variance. Except for CH, left PW, and volume, all other parameters were significant predictors of age ($p < 0.05$). In males, CL showed the strongest explanatory value ($F = 67.719$; $p < 0.001$), accounting for 17.1% of age variation. All parameters except HL and HU max were significant predictors of age in males ($p < 0.05$).

Table 6
Linear regression analyses in both sexes

Parameter	Sex	Constant (B0)	Coefficient (B1)	Std. Error	%95 Confidence Interval (CI)	R^2	F	p
CL	Female	-4.07	2.339	0.483	1.390–3.288	0.067	23.487	**< 0.001**
	Male	-40.544	3.341	0.406	2.542–4.140	0.171	67.719	**< 0.001**
CH	Female	38.247	1.023	0.728	-0.409–2.455	0.006	1.161	0.161
	Male	31.579	1.437	0.673	0.144–2.761	0.014	4.465	**0.033**
Left PW	Female	38.983	1.676	1.53	-1.334–4.685	0.004	1.2	0.274
	Male	8.978	6.745	1.208	4.367–9.122	0.087	31.15	**< 0.001**
Right PW	Female	28.201	3.772	1.594	0.636–6.909	0.017	5.598	**0.019**
	Male	7.533	6.865	1.209	4.487–9.243	0.09	32.257	**< 0.001**
Left DW	Female	27.696	4.403	1.462	1.527–7.279	0.027	9.069	**0.003**
	Male	26.958	4.424	1.29	1.887–6.962	0.035	11.762	**0.001**
Right DW	Female	29.148	4.142	1.594	1.006–7.278	0.02	6.753	**0.01**
	Male	23.72	5.117	1.289	2.640–7.713	0.047	16.122	**< 0.001**
Left CML	Female	-11.329	2.08	0.388	1.318–2.843	0.081	28.797	**< 0.001**
	Male	15.888	0.987	0.315	0.366–1.607	0.029	9.794	**0.002**
Right CML	Female	-23.084	2.462	0.376	1.722–3.201	0.116	42.888	**< 0.001**
	Male	12.823	1.07	0.328	0.426–1.714	0.032	10.672	**0.001**
HL	Female	-10.202	1.667	0.377	0.926–2.408	0.056	19.581	**< 0.001**
	Male	29.862	0.443	0.335	-0.216–1.102	0.056	19.581	0.187
HU max	Female	74.389	-0.002	0.004	-0.030 – -0.014	0.075	26.626	**< 0.001**
	Male	49.596	-0.002	0.005	-0.012–0.009	0	0.085	0.77
Volume (mm^3)	Female	34.358	0.008	0.004	0.000–0.015	0.012	4.018	**0.046**
	Male	4.307	0.017	0.002	0.012–0.021	0.155	60.038	**< 0.001**
HU Mean	Female	94.845	-0.14	0.014	-0.169 – -0.112	0.224	94.426	**< 0.001**
	Male	67.817	-0.055	0.017	-0.089 – -0.020	0.002	9.831	**0.002**

Following univariate linear regression analysis, separate stepwise multivariate regression models were developed for each sex. The stepwise method was used to reduce the risk of multicollinearity, and only variables that independently contributed to age prediction were retained in the final models.

In females, fusion stage, mean HU, and right CML were retained in the final model. The model was statistically significant ($F(3,326) = 99.083$; $p < 0.001$) and explained 47.7% of the variation in age ($R^2=0.477$; adjusted $R^2=0.472$). The strongest predictor was fusion stage (positive effect, $\beta = 0.406$), followed by mean HU (negative effect, $\beta=-0.382$) and right CML (positive effect, $\beta = 0.264$). All independent variables contributed significantly to the model ($p < 0.05$).

In males, fusion stage, volume, and CL were retained in the final model. This model was also statistically significant ($F_{(3,325)} = 60.932$; $p < 0.001$) and explained 36% of age variation ($R^2=0.360$; adjusted $R^2=0.354$). Fusion stage made the strongest contribution to age prediction ($\beta = 0.433$), followed by volume ($\beta = 0.165$) and CL ($\beta = 0.138$). All independent variables were significant contributors to the model ($p < 0.05$). The equations derived from the stepwise multiple regression analyses are provided below.

Estimated Age $_{(FEMALE)}$ = 13,665 + (9,235 x Fusion stage) – (0,113 x HU mean) + (1,907 x right CML)

Estimated Age $_{(MALE)}$ = -16,467 + (9,046 x Fusion stage) + (0,007 x Volume) + (1,113 x CL)

Discussion

Anthropometric analysis of the hyoid bone has been widely used for sex and age estimation. Most previous studies have relied on direct measurements from autopsy specimens or anatomical collections, as well as photographs of isolated hyoid bones [4, 6–8]. Other studies have used two-dimensional computed tomography (CT) images from imaging databases [9, 10], three-dimensional bone reconstructions [5, 11, 12], or direct radiographs obtained from different projections [13].

The absence of stage-0 fusion after the age of 30 and the progressive increase in fusion stage with advancing age in our study are consistent with previous literature. However, bilateral complete fusion (stage 3) reached its highest frequency in the 71–80 age group at 47% and did not occur in all older individuals. This finding is in line with data from the Turkish population reported by Balseven-Odabaşı et al. and with the view of Urbanová et al. that hyoid fusion alone has limited value for age estimation [4, 10]. Although complete fusion is generally reported to be rare during adolescence and young adulthood [5, 14, 15], the presence of stage-3 fusion in one case aged 15–18 years in our study is noteworthy. This finding is compatible with a national case report involving a 16-year-old individual [16] and with studies from the Indian population suggesting that fusion may begin during adolescence [17, 18]. As also indicated by Köse et al. [19], such early exceptional cases demonstrate the broad biological variability of hyoid bone fusion.

In our study, all morphometric measurements except the distal width (DW) parameters were significantly greater in males than in females, consistent with previous reports in the literature [3, 4]. Evaluation across age groups showed that morphological development of the hyoid bone was largely completed by young adulthood, around the age of 30, with no significant differences observed among older age groups. This suggests that post-30 changes are more likely attributable to individual variation than to age-related progression. The finding that morphometric dimensions continue to increase until approximately 30 years of age is also supported by existing literature [6, 8, 20, 21].

The combined discriminant function model in our study achieved an overall sex estimation accuracy of 93.8% (91.8% in males and 95.8% in females), which is higher than the rates reported for traditional approaches in the literature (73%–88.2%) [1, 6, 7]. The only CT-based study reporting a slightly higher accuracy was conducted by Torimitsu et al. [9], with a rate of 94.6%. The small difference between these results may be attributable to the substantially larger sample size

in our study (n = 660 vs. n = 280) and to inter-population variation. The fact that CL and HL were among the most significant variables for sex discrimination in both our study and the Japanese population study further supports their consistent relevance in the literature.

Fakhry et al. [22], who examined sexual dimorphism of the hyoid bone using three-dimensional geometric morphometry, also reported larger hyoid dimensions in males, supporting our findings. They suggested that cadaveric measurements may be greater than live CT measurements because postmortem loss of muscular tension alters the position and configuration of the hyoid bone, and they emphasized that the hyoid is a dynamic structure affected by functional and biomechanical factors. Unlike Fakhry et al. [22], who found no significant effect of age on hyoid morphology, our results showed morphometric increase until young adulthood followed by relative stability in older age groups. This discrepancy may be related to differences in sample size, age distribution, and analytical approach between studies.

In our study, hyoid bone volume obtained through three-dimensional segmentation was significantly greater in males (mean 2614.03 mm^3) than in females (mean 1710.16 mm^3) and showed a positive correlation with age. Among univariate discriminant variables, volume yielded the highest sex classification accuracy (92.7% in males and 82.4% in females). These findings are largely consistent with another Turkish population study that used 3D Slicer™ and the same 130 HU threshold, reporting mean volumes of 2609.6 mm^3 in males and 1579.9 mm^3 in females [23]. By contrast, Ito et al. [12] reported substantially higher volume values, lower classification accuracy (55% in males and 79% in females), and no significant correlation with age in a Japanese population. These differences likely reflect both population-specific variation and methodological differences. In the present study, segmentation was optimized by manually including low-HU medullary areas on each slice, whereas the workflow details reported by Ito et al. [12] were limited.

Unlike conventional studies that measure radiodensity within a limited region of interest, our study calculated radiodensity from the entire hyoid bone using three-dimensional segmentation. Mean radiodensity was significantly higher in males (370.63 HU) than in females (337.6 HU). Radiodensity showed a slight increase between ages 15 and 30, followed by a gradual decline in older age groups; this decline was particularly evident in females, where mean HU explained 22.4% of age variation. The higher female classification rate obtained using mean HU in univariate discriminant analysis (63.3% in females and 55.8% in males) is directionally consistent with Fisher et al. [5], who also used a 3D hyoid model (69% in females and 59% in males). The numerical differences between studies may be related to sample size (n = 660 vs. n = 136). The marked age-related decrease in radiodensity among females, consistent with Fisher et al. [5], may be associated with postmenopausal hormonal changes and the resulting reduction in bone tissue quality.

Age estimation in our study was performed using a two-stage regression approach that simultaneously evaluated fusion stage, morphometry, volume, and radiodensity. The resulting multivariate models explained 36% of age variation in males and 47.7% in females. To our knowledge, no previous age estimation model has incorporated these four analytical components together. Comparable studies used different strategies: Naimo et al. [15] classified broad age groups in an Australian population with 87.7% accuracy using morphometric measurements alone, whereas Urbanová et al. [10] analyzed cadavers from a Czech population by grouping cases into predefined age categories (< 30, 31–50, 51–70, and > 71 years). The lower explanatory values in our study therefore reflect a fundamental methodological difference. Rather than assigning individuals to artificial age categories, we estimated age as a continuous variable. Accordingly, the inclusion of biomechanical parameters such as volume and radiodensity provides a more objective framework for individual age estimation than population-based categorical classification alone.

Conclusion

This study provides a comprehensive CT-based forensic identification model by evaluating hyoid bone morphometry, volume, radiodensity, and fusion status together in a large Turkish population sample (n = 660). The combined discriminant function model achieved high sex estimation accuracy (93.8%; 91.8% in males and 95.8% in females), demonstrating that the hyoid bone shows marked sexual dimorphism in this population and represents a valuable biological indicator for forensic identification. The prominence of volume, corpus length (CL), and anteroposterior length (HL) in the analyses further indicates that sexual dimorphism is not limited to linear measurements but is also closely related to the three-dimensional size of the bone. These findings support the forensic applicability of CT-based segmentation and volumetric analysis. Although hyoid fusion showed an age-related pattern, including the absence of stage-0 fusion after the age of 30, bilateral complete fusion was observed in only 47% of individuals aged 71–80 years. Therefore, fusion status should not be used as a standalone age criterion, as fusion may remain incomplete even in older individuals.

The main contributions of this study are as follows:

- demonstrating high sex estimation accuracy (93.8%) using hyoid bone parameters,
- showing that the absence of stage-0 fusion after age 30 may help distinguish individuals younger and older than this threshold,
- developing multiparametric age estimation models that explained 47.7% of age variation in females and 36% in males,
- establishing a population-specific anthropometric and radiodensity dataset for the Turkish population.

In conclusion, a three-dimensional segmentation-based multiparametric approach that integrates morphometry, volume, radiodensity, and fusion provides more objective, reliable, and population-specific information than assessment of any single hyoid bone parameter alone. While this approach is particularly robust for sex estimation, age estimation should preferably be interpreted as an estimated age range rather than an exact chronological age.

Declarations

Ethics Approval:

This study was performed in line with the principles of the Declaration of Helsinki. Approval was granted by the Ethics Committee of Gulhane Scientific Research (Date: 06.05.2025. No: 251).

Competing Interests:

The authors have no competing interests to declare that are relevant to the content of this article.

Funding:

The authors did not receive support from any organization for the submitted work.

Author Contribution

Data Curation & Case Screening: D.G.Ç., H.B.Investigation (Radiological Measurements): D.G.Ç., H.B., S.Ö., U.B.Validation & Quality Control: S.Ö., U.B.Visualization (Figures 1–4): B.K.Writing – Original Draft: D.G.Ç., H.B., B.K.Writing – Review & Editing: D.G.Ç., H.B., S.Ö., U.B., B.K.All authors reviewed the manuscript.

Data Availability

The datasets generated and analysed during the current study are not publicly available due to privacy and ethical restrictions regarding forensic case data and radiological images. However, the de-identified data are available from the corresponding author on reasonable request.

References

1. Haj Salem N, Amine Mesrati M, Belhadj M, Saadi S, Ben Jomaa S, Ouelha D et al (2020) Age estimation and sex determination by CT-scan analysis of the hyoid bone: Application on a Tunisian population. Revue de Med Legale 11(4):137–144
2. Auvenshine RC, Pettit NJ (2020) The hyoid bone: an overview. Cranio - J Craniomandib Pract 38(1):6–14
3. Keven A, Öztürk Bostancı S, Aytaç G, Sindel M (2024) Identification of hyoid bone morphometry in terms of gender in the Turkish population. Anatomy 18(2):61–65
4. Balseven-Odabasi A, Yalcinozan E, Keten A, Akçan R, Tumer AR, Onan A et al (2013) Age and sex estimation by metric measurements and fusion of hyoid bone in a Turkish population. J Forensic Leg Med 20(5):496–501
5. Fisher E, Austin D, Werner HM, Chuang YJ, Bersu E, Vorperian HK (2016) Hyoid bone fusion and bone density across the lifespan: prediction of age and sex. Forensic Sci Med Pathol 12(2):146–157
6. Kim DI, Lee UY, Park DK, Kim YS, Han KH, Kim KH et al (2006) Morphometrics of the hyoid bone for human sex determination from digital photographs. In: J Forensic Sci. p. 979–984
7. Kindschuh SC, Dupras TL, Cowgill LW (2010) Determination of sex from the hyoid bone. Am J Phys Anthropol 143(2):279–284
8. Mukhopadhyay PP (2010) Morphometric features and sexual dimorphism of adult hyoid bone: A population specific study with forensic implications. J Forensic Leg Med 17(6):321–324
9. Torimitsu S, Makino Y, Saitoh H, Ishii N, Yajima D, Inokuchi G et al (2018) Determination of sex on the basis of hyoid bone measurements in a Japanese population using multidetector computed tomography. Int J Legal Med 132(3):907–914
10. Urbanová P, Hejna P, Zátopková L, Šafr M (2013) What is the appropriate approach in sex determination of hyoid bones? J Forensic Leg Med 20(8):996–1003
11. Morávek A, Henyš P, Harnádková K, Kuchař M, Endlicher R, Prstková K et al Bone mineral radio density as a sex estimation feature on an example of hyoid bones Short title: BMD as sexual differentiating factor [Internet]. Available from: https://ssrn.com/abstract=4983150
12. Ito K, Ando S, Akiba N, Watanabe Y, Okuyama Y, Moriguchi H, Shimada M (2012) Morphological study of the human hyoid bone with three-dimensional CT images—Gender difference and age-related changes—. Okajimas Folia Anat Jpn 89(3):83–92
13. Reesink EM, Van Immerseel AAH, Brand R, Bruintjes TD (1999) Sexual Dimorphism of the Hyoid Bone? Int J Osteoarchaeology Int J Osteoarchaeol
14. By B, Parsons FG (1908) Journal Of Anatomy And Physiology The Topography And Morphology of The Human Hyoid. IV. Proeeedinys Anatomical Society
15. Naimo P, O'Donnell C, Bassed R, Briggs C (2015) The use of computed tomography in determining development, anomalies, and trauma of the hyoid bone. Forensic Sci Med Pathol 11(2):177–185
16. Mutlu GD, Aşırdizer M, Kartal E, Keskin S, Mutlu İ, Göya C (2024) Type and Fusion Identification by Age and Sex in Human Hyoid Bone Using 3D CT Images in a Turkish Sample. Eastern J Med 29(4):446–454

17. Harjeet K, Synghal S, Kaur G, Aggarwal A, Wahee P (2010) Time of fusion of greater cornu with body of hyoid bone in Northwest Indians. Leg Med 12(5):223–227
18. Gupta A, Kohli A, Aggarwal NK, Banerjee KK (2008) Study of age of fusion of hyoid bone. Leg Med 10(5):253–256
19. Köse E, Göller Bulut D (2022) The use of hyoid bone dimensions in age and sex estimation in a Turkish population: a cone-beam computed tomography study. Folia Morphol (Warsz) 81(1):183–189
20. Miller KWP, Walker PL, O'Halloran RL (1998) Age and sex-related variation in hyoid bone morphology. J Forensic Sci 43(6):1138–1143
21. Tarifi AA, Sarhan SZ, Mousa; AA, Al Safarini AD, Mustafa DF et al (2023) Radiological Morphometric Study of the Hyoid Bone using Three-Dimensional Computed Tomography (3D-CT) Scans Estudio Morfométrico Radiológico del Hueso Hioides Mediante Tomografía Computarizada Tridimensional (3D-CT). Int J Morphol
22. Fakhry N, Puymerail L, Michel J, Santini L, Lebreton-Chakour C, Robert D et al (2013) Analysis of hyoid bone using 3D geometric morphometrics: An anatomical study and discussion of potential clinical implications. Dysphagia 28(3):435–445
23. Gurlek Celik N, Oktay M (2025) Evaluation of hyoid bone position, shape, area, volume, and tongue volume. Surg Radiol Anat. ;47(1)

Figures

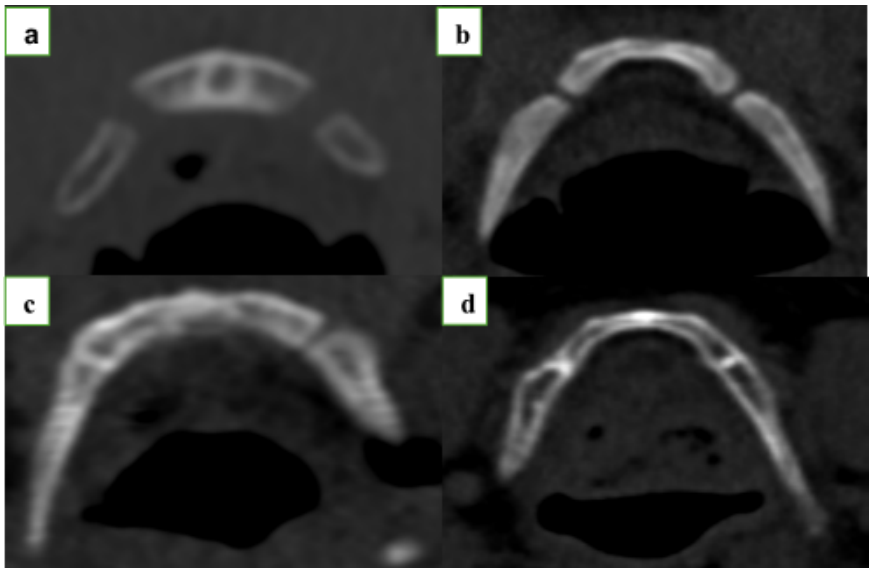

Figure 1

Fusion stages according to the system established by Fischer et al. [5] A: stage 0 (joint space > 2.5 mm), B: stage 1 (joint space < 2.5 mm), C: stage 2 (partial/unilateral fusion), D: stage 3 (complete fusion)

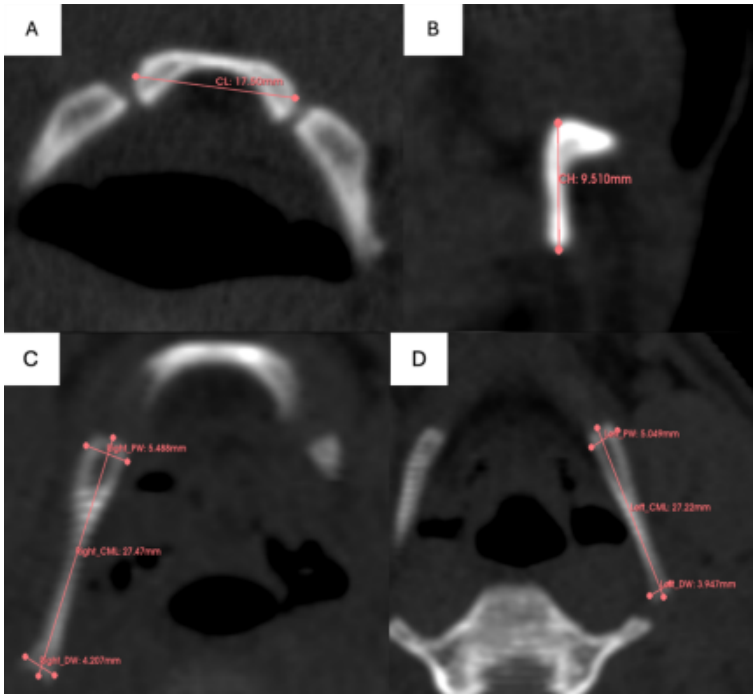

Figure 2

Osteometric measurements. A: corpus length (CL). B: corpus height (CH). C: proximal and distal end widths and length of the right greater cornu (PW, DW, CML). D: proximal and distal end widths and length of the left greater cornu (PW, DW, CML)

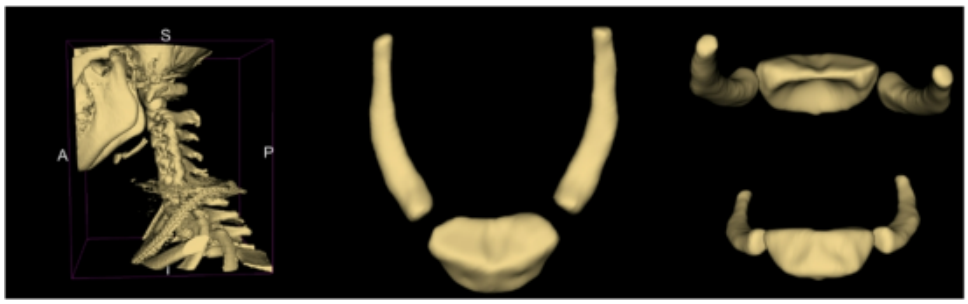

Figure 3

Views of the three-dimensional model of the head and neck skeleton and the isolated hyoid bone from different angles.

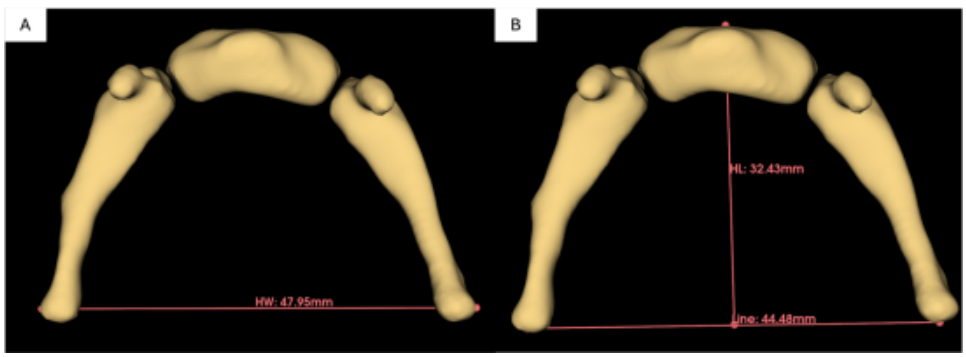

Figure 4

Measurements performed after three-dimensional segmentation. A: maximum width of the hyoid bone (HW). B: anteroposterior length of the hyoid bone (HL)